Alginate-based complex fibers with the Janus morphology for controlled release of co-delivered drugs

Wing-Fu Lai , Eric Huang , Kwok-Ho Lui

PII: S1818-0876(20)30284-1
DOI: https://doi.org/10.1016/j.ajps.2020.05.003
Reference: AJPS 647

To appear in: *Asian Journal of Pharmaceutical Sciences*

Received date: 10 March 2020
Revised date: 12 May 2020
Accepted date: 25 May 2020

Please cite this article as: Wing-Fu Lai , Eric Huang , Kwok-Ho Lui , Alginate-based complex fibers with the Janus morphology for controlled release of co-delivered drugs, *Asian Journal of Pharmaceutical Sciences* (2020), doi: https://doi.org/10.1016/j.ajps.2020.05.003

Title page

Alginate-based complex fibers with the Janus morphology for controlled release of co-delivered drugs

Wing-Fu Lai[a,b,*], Eric Huang[b], Kwok-Ho Lui[b]

[a] School of Life and Health Sciences, The Chinese University of Hong Kong (Shenzhen), Shenzhen 518172, China

[b] Department of Applied Biology and Chemical Technology, Hong Kong Polytechnic University, Hong Kong Special Administrative Region, China

*Corresponding author. School of Life and Health Sciences, The Chinese University of Hong Kong (Shenzhen), Shenzhen 518172, China. Tel.: +86 0755 23519010

E-mail: rori0610@graduate.hku.hk (W.F. Lai)

Graphical Abstract

Alginate-based complex fibers with the Janus morphology were generated using a one-pot method and were shown to demonstrate the capacity of enabling the release profile of each of the co-delivered drugs to be precisely manipulated.

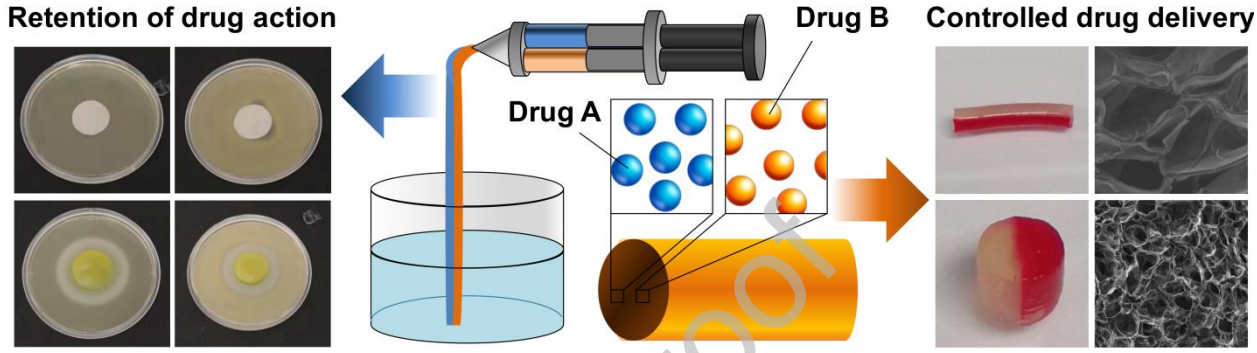

Abstract

Hydrogels are soft materials consisting of a three-dimensional network of polymer chains. Over the years, hydrogels with different compositions have been developed as drug carriers for diverse biomedical applications, ranging from cancer therapy and wound care to the treatment of neurodegenerative and inflammatory conditions. Most of these carriers, however, are designed only to deliver single agents. Carriers based on hydrogels for enabling co-delivery of multiple agents, with the release rate of each of the co-delivered agents to be tuned individually, are lacking. This study reports a one-pot method of fabricating alginate-based complex fibers with the Janus morphology, with carboxymethyl cellulose sodium as a polymeric modifier of the properties of each of the fiber compartments. By using malachite green and minocycline hydrochloride as model drugs, the generated fibers demonstrate the capacity of enabling the release profile of each of the co-delivered drugs to be precisely controlled. Along with their negligible toxicity and the retention of the

activity of the loaded drugs, the complex fibers reported in this study warrant further development and optimization for applications that involve co-delivery of multiple agents.

Keywords:

Janus morphology; Complex fiber; Tunable release profiles; Co-delivery; Controlled release

1. Introduction

Hydrogels are soft materials that have been widely studied in the literature as drug carriers for diverse biomedical applications, ranging from cancer therapy [1] and wound care [2] to the treatment of neurodegenerative [3] and inflammatory conditions [4]. Among different polymers exploited for hydrogel fabrication, carbohydrate polymers (e.g., alginic acid, chitosan, dextran, cellulose and starch) have gained special interest, partly owing to their high biocompatibility and abundance in nature. Over the years, different gel-based systems have been fabricated by using these polymers for biomedical use [5-10]. For example, the gel formed from a blend of chitosan and carboxymethyl cellulose sodium (CMC-Na) has been utilized for cutaneous administration of vitamin E to protect the skin from UV damage and to achieve moisturizing effects [11]. Nanoparticles have also been generated via polyelectrolyte complexation of sodium alginate (Na-Alg) with poly(ethylenimine)-graft-polysorbate [12]. The nanoparticles show responsiveness to the ionic strength of the surrounding medium, and enable controlled delivery of protein drugs. More recently, with the use of poloxamer407 (P407) and CMC-Na, the development of a composite gel has been reported for the delivery of the Cortex Moutan extract [13]. The extract-loaded gel has been used in transdermal functionalized textile therapy for the treatment of atopic dermatitis [13]. Not only have all these advances evidenced the promising potential of carbohydrate polymers in drug delivery, but they have also enhanced the effectiveness and bioavailability of therapeutic agents in practice.

Na-Alg is one of the carbohydrate polymers that have received intense attention in biomedical research [14, 15]. It is a naturally occurring polysaccharide consisting of guluronic (G) and mannuronic (M) acid residues [16, 17], with the G-blocks and

M-blocks interspersed within regions of alternating structures [16, 18]. As drug carriers, Alg-based materials can be fabricated in multiple forms, ranging from nanoparticles to fibers [12, 19]. The latter has attracted particular interest because fibers cannot only carry drug molecules but may also serve as building blocks to generate scaffolds to allow the adherence, proliferation and differentiation of cells in the treatment of pathological or injured tissues [19-22]. Despite this promising potential and similar to the case of other drug carriers, Alg-based fibers documented in the literature have been reported predominately for delivery of single agents till now [23-26]. As a matter of fact, while the “single molecule, single target, and single drug" approach dominates for most of the 20th century [27], multi-drug therapy has gained increasing attention due to its potential of boosting the therapeutic efficiency beyond that of a single drug [28-30]. Although few efforts in the literature have attempted to mix and load different drugs into a single system (ranging from polymeric micelles [31, 32] and metal-organic frameworks [33] to hydrogels [34, 35]) for co-delivery of multiple drugs, most of these efforts fail to enable precise manipulation of the release rate of each of the co-delivered drugs because changing the release sustainability of the system for one drug leads to changes in the release profile of the other. This limits the possibility of co-delivering therapeutic agents that show different desired release kinetic patterns. To address this need, this study reports a one-pot method of generating alginate-based complex fibers with the Janus morphology, with CMC-Na as a polymeric modifier of the properties of each of the fiber compartments. The generated fibers show high biocompatibility, and are applicable to applications in which co-delivery of multiple drugs at individual release rates is required.

2. Materials and methods

2.1. Materials

CMC-Na (average Mw ≈ 10 kDa, degree of substitution = 0.7), minocycline hydrochloride (MH), and malachite green (MG) were purchased from Sigma-Aldrich (St. Louis, MO, USA). Na-Alg (40-90 mPa·s in 1% aqueous solution, M/G ratio of 2.05, Mw = 16-34 kDa) was purchased from Fisher Scientific Co. (Pittsburgh, PA). Calcium chloride ($CaCl_2$) was purchased from Macklin (Shanghai, China). Dulbecco's Modified Eagle's Medium (DMEM; Gibco, Grand Island), fetal bovine serum (FBS, Hangzhou Sijiqing Biological Engineering Materials Co., China) and penicillin G-streptomycin sulfate (Life Technologies Corporation. USA) were adopted as the cell culture medium. Trypsin-EDTA (0.25% trypsin-EDTA) was purchased from Invitrogen (Carlsbad, CA, USA).

2.2. Fabrication of complex fibers with the Janus morphology

A syringe barrel having two chambers located side by side was designed and adopted for the generation of Janus fibers. Each chamber was filled with an aqueous solution containing appropriate amounts of Na-Alg, CMC-Na and a drug model. The Na-Alg/CMC-Na blend was designated as AxCy, with the mass-to-mass ratio of Na-Alg and CMC-Na being x/y. A syringe pump was used to push the two-piece plunger rod, in which a rubber piston was attached to the end of each piece, to eject the solutions from the dual-barrel syringe into a collection bath containing a 10% (w/v) solution of $CaCl_2$. The diameter of the generated fiber was controlled by changing the size of the syringe nozzle adopted. The Janus fibers were collected after 10 min of gelation at ambient conditions in the collection bath, and were sterilized by UV irradiation. The same procedure was adopted to generate fibers with a homogenous composition by loading the two barrels of the syringe with the same polymer solution. The composition of the complex fiber was designated as C-AxCy, with the

mass-to-mass ratio of Na-Alg and CMC-Na being x/y.

2.3 Thermogravimetric analysis (TGA)

TGA profiles of Na-Alg, CMC-Na, and C-A1C3 were obtained using a Q50 TGA analyzer (TA Instruments, New Castle, Delaware, USA) equipped with platinum pans. The profiles were collected in an inert atmosphere of nitrogen from 40 to 600 ^{o}C. The heating rate was uniform at 10 ^{o}C/min throughout analysis.

2.4 Scanning electron microscopy (SEM)

The microstructure of the lyophilized fiber was examined using a JEOL JSM-6380 microscope (Tokyo, Japan) operated at an accelerating voltage of 10 kV. Before SEM analysis, the sample was sputter-coated with gold.

2.5 Evaluation of the mechanical and rheological properties

Tensile tests were conducted under strain control at a rate of 0.1 mm/s using an *in situ* bidirectional tension-compression testing system (IBTC-300). Viscosity parameters of Na-Alg/CMC-Na blends with different mass-to-mass ratios of Na-Alg and CMC-Na was measured using Brookfield DV-III Ultra programmable rheometer (Brookfield Engineering Laboratories Inc., Middleboro, MA, USA) with spindles (CP-40). Measurements were performed at different shear rates at ambient conditions, with the equilibration time at every shear rate being 15 s. Viscoelastic properties of the blends, before and after gelation, were examined in the frequency range from 0.1 to 100 rad/s. The storage modulus (G') and loss modulus (G'') were determined.

2.6 Determination of the swelling capacity

0.05 g of a lyophilized complex fiber was immersed in 100 ml of simulated body fluid. At a pre-set time interval, the fiber was retrieved by centrifugation for 5 min at a relative centrifugal force of 4000 × g, followed by the removal of the supernatant. The water absorption ratio (WAR) and water content of the fiber were calculated using the

following formulae:

$$WAR = \frac{m_s - m_d}{m_d} \quad (1)$$

$$Water\ content\ (\%) = \frac{m_s - m_d}{m_s} \times 100\ \% \quad (2)$$

Where m_s and m_d represent the mass of the swollen fiber and the mass of the dried fiber, respectively.

2.7 Cytotoxicity assay

3T3 mouse fibroblasts and HEK293 cells were cultured in DMEM supplemented with 10% FBS, 100 UI/ml penicillin, 100 μg/ml streptomycin, and 2 mM L-glutamine. 24 h before the assay, cells were seeded in a 96-well plate at an initial density of 5000 cells per well, and were incubated under a humidified atmosphere of 5% CO_2 at 37 °C. During the assay, polymer solutions with different concentrations were prepared by dissolving appropriate amounts of Na-Alg (or CMC-Na) in the fresh cell culture medium. The growth medium in each well was replaced with 100 μL of the polymer solution. After 5-h incubation at 37 °C, the polymer solution was replaced with the fresh growth medium. The CellTiter 96 AQueous non-radioactive cell proliferation assay (MTS assay; Promega Corp., Madison, WI) was performed, according to the manufacturer's instructions, either immediately or after 24 h of post-treatment incubation. Apart from using the MTS assay, changes in cell proliferation upon 5-h treatment with the polymer solution, with or without subsequent 24 h of post-treatment incubation, were examined by counting the number of viable cells using a CASY Cell Counter and analyzer system (Casy Roche Innovativs model TT, Reutlingen, Germany).

2.8 Determination of the hemolytic activity

Female New Zealand White rabbits were purchased from Guangdong Medical

Laboratory Animal Center (Guangzhou, China). During assay, blood was collected from the marginal ear vein into a heparin-containing tube, followed by centrifugation at 2000 × g for 10 min at 4 °C. All procedures were approved by the Ethical Committee of the Hong Kong Polytechnic University. The collected erythrocytes were washed with PBS (pH 7.4) until the supernatant was colorless. An appropriate amount of a lyophilized complex fiber was ground in PBS using mortar and pestle, and the solution obtained was filtered before use. Erythrocytes were added to the filtrate until a final concentration of 8% (v/v) was attained. After incubation at 37°C for one h, the mixture was centrifuged at 2000 × g for 15 min. The absorbance of the supernatant was recorded at 414 nm. The extent of hemolysis in PBS and 0.1% Triton X-100 was defined as 0% and 100%, respectively.

2.9 Determination of the drug encapsulation efficiency

Complex fibers loaded with a model drug were generated as usual. The $CaCl_2$ solution was collected from the collection bath. The concentrations of MG and MH in the solution were determined at 617 nm and 350 nm, respectively, using a UV/Vis spectrophotometer (Varian, Inc., USA). The encapsulation efficiency (EE) was calculated using the following equation:

$$EE\ (\%) = \frac{m_T - m_F}{m_T} \times 100\ \% \quad (3)$$

where m_T is the total mass of the drug added during the drug loading process, and m_F is the mass of the drug remained in the collection bath.

2.10 Drug release evaluation

After fabrication and lyophilization of a drug-loaded complex fiber, 20 ml of simulated body fluid was added to the fiber. At a pre-set time interval, 0.2 ml of the buffer solution was removed for testing, and was replaced with 0.2 ml of simulated body fluid. The amount of the drug released from the fiber was determined using a

UV/Vis spectrophotometer (Varian, Inc., USA). The cumulative percentage of drug release was calculated using the following formula:

$$Cumulative\quad drug\quad release\quad (\%) = \frac{\sum_{t=0}^{t} m_t}{m_\infty} \times 100\ \% \tag{4}$$

Where m_t is the mass of the drug released from the fiber at time t, and m_∞ is the mass of the drug loaded into the fiber.

2.11 Antibacterial test

An aqueous solution containing appropriate amounts of Na-Alg, CMC-Na, and MH was poured into a collection bath containing a 10% (w/v) solution of $CaCl_2$. The gel was collected after 10 min of gelation at ambient conditions in the collection bath. It was cut into a shape of a column (diameter = 1.5 cm, height = 0.3 cm), and was sterilized by UV irradiation. Either *Staphylococcus aureus* or *Escherichia coli* was swabbed on a Luria broth (LB) agar plate. After placing the gel in the plate and incubating the plate for 24 h at 37 °C, photos were taken. The zone of inhibition was measured to determine the growth of bacteria around the gel.

2.12 Statistical analysis

All data were expressed as the means ± standard deviation. Statistical analysis was conducted using a one-way analysis of variation (ANOVA), followed by the Tukey's honestly significant difference (HSD) test for multiple comparisons. Differences with $P < 0.05$ were considered to be statistically significant.

3. Results and discussion

3.1. Design and fabrication of complex fibers with the Janus morphology

Complex fibers with the Janus morphology are generated via ionic gelation of Na-Alg using the set-up shown in **Fig. 1**. To manipulate the properties of the generated fibers, CMC-Na is employed as a polymeric modifier. Earlier studies have shown that

solutions of CMC-Na are more effective than solutions of other anionic polysaccharides (e.g., xanthan gum and Na-Alg) in preventing the sedimentation of mixed agents [36]. Addition of CMC-Na can, therefore, allow the drug-loaded Na-Alg solution to be more homogenous during fiber fabrication in this study, and can facilitate the production of fibers in which drug molecules are evenly distributed. Apart from this, both Na-Alg and CMC-Na are FDA-approved polymeric materials for biomedical and food applications [37-39]. They are biodegradable and non-toxic [39-41], and can hence ensure that the fibers generated in this study are safe for use in the preclinical and clinical contexts.

The high safety profile of the fiber constituents (viz., Na-Alg and CMC-Na) is confirmed by the MTS assay performed in 3T3 fibroblasts and HEK293 cells. 3T3 mouse fibroblasts are selected because the viable rates of these cells are reported to be substrate-dependent [42]. They have been used in the literature to evaluate the cytotoxicity of an agent of interest [42]. On the other hand, HEK293 cells are one of the widely adopted cell lines in drug toxicology studies [43], especially in assessing the toxic effect of a drug candidate on the renal system [44]. They are, therefore, utilized in this study as a cell model for assessing the cytotoxicity of Na-Alg and CMC-Na. No apparent loss of cell viability (and hence no acute cytotoxicity) is noted after 5 h of treatment of the cells with either Na-Alg or CMC-Na (**Fig. 2A**). To determine possible chronic cytotoxicity displayed by the fiber constituents, the viability of the treated cells is assayed after a 24-h post-treatment incubation. No observable cytotoxicity is found in all concentrations tested. Apart from the MTS assay, the proliferation of the cells is assessed by cell counting, and is found not to be affected by treatment with either Na-Alg or CMC-Na, regardless of the presence or absence of the subsequent post-treatment incubation (**Fig. 2B**). Along with their high

biocompatibility as revealed by the low hemolytic rates (< 1%) (**Fig. 2C**), the fiber constituents (and thus the fibers generated) demonstrate adequate safety for use in drug delivery.

3.2 Thermal and mechanical properties of complex fibers

Thermal properties of the fiber constituents and the complex fiber are studied using TGA (**Fig. 2D**). A weight loss is observed up to 110 °C in all TGA profiles, owing to the presence of moisture in the samples. The rupture of the chains and fragments leads to one weight loss at 215-270 °C in the TG curve of Na-Alg. On the other hand, due to the decomposition of CMC-Na and hence the loss of CO_2, a rapid weight loss is observed at 260-320 ^{o}C in the TG curve of CMC-Na. These two weight loss steps combine in the TG curve of the C-A1C3 fiber, leading to a weight loss at 210-320 ^{o}C. These results reveal that the properties of the fiber are contributed by both Na-Alg and CMC-Na.

The microstructure of the complex fiber is examined by SEM (**Fig. 3A**). All fibers show porous structures. The tensile stress-strain behavior of the fibers is presented in **Fig. 3B**, which shows that the complex fibers possess high stretchability under a tensile force in the magnitude of kilopascals. The fracture strain of the fiber is reduced by increasing the amount of CMC-Na added, with the fiber consisting of C-A1C0 displaying the highest fracture strain. Apart from the mechanical strength, the rheological properties of the fibers are studied. The apparent viscosity of the tested Na-Alg/CMC-Na blends at a low shear rate is higher than that at a high shear rate (**Fig. 3C**). This suggests that the blends display pseudoplastic behavior. Due to the high viscosity of the CMC-Na solution, the viscosity of the blend is increased with the mass percentage of CMC-Na. The viscoelastic parameters (i.e., G' and G'') of the Na-Alg/CMC-Na blends are examined after ionic gelation with Ca^{2+} ions (**Fig.**

3D-3E). In all samples tested, the G' values are higher than G''. This indicates that upon interactions with Ca^{2+}, the elastic behavior of the blends predominates over the viscous behavior. In addition, the values of both G' and G'' are negatively related to the mass percentage of CMC-Na, suggesting that the addition of the modifier can reduce the mechanical rigidity of the fiber formed.

Finally, the swelling capacity of a complex fiber depends predominately on the amount of fluids the fiber can take up upon hydration. It is determined in this study based on the WAR value and the water content. These two values have been widely adopted by other studies as indicators of the swelling capacity [45-47]. Results reveal that the WAR value and water content of the fiber are positively related to the mass percentage of CMC-Na (**Fig. 4**).

3.3 Performance in drug encapsulation and release

To evaluate the EE and release sustainability of the fibers, MG and MH are adopted as the drug models. MG is a triphenylmethane dye used in the aquaculture industry as a fungicide and an ectoparasiticide [48]; whereas MH is a semisynthetic tetracycline derivative showing broad-spectrum antibiotic effects [49]. The maximum UV/Vis absorption peak of MG (617 nm) is at a wavelength that is minimally absorbed by MH (**Fig. 5A**). The same also applies to the absorption peak of MH at 350 nm, at which absorption by MG is negligible. This enables more accurate characterization of the release profiles of MG and MH in the later part of this study when the two drug models are co-delivered by the fiber. By controlling the diameter of the nozzle of the syringe adopted, fibers with different diameters can be generated. The impact of the fiber diameter on the EE of the fiber is found to be insignificant (**Fig. 5B**); however, the fiber with a diameter of 15 mm has a substantially lower rate of drug release compared to that with a diameter of 3.5 mm (**Fig. 5C**). This is attributed to the

decrease in the surface area-to-volume ratio of the fiber when the fiber diameter is increased, leading to a lower rate of drug diffusion.

The impact of the mass percentage of CMC-Na on the EE and drug release sustainability of the fiber is investigated, too. The EE of the tested fibers is estimated to be around 80%-90%. The mass percentage of CMC-Na does not have a significant influence on the overall efficiency of the fiber in drug encapsulation (**Fig. 6A**). During drug release, water in the gel matrix is the medium through which drug molecules diffuse [45]. The trend of changes in the rate of drug release is, therefore, expected to follow that of changes in the swelling capacity of the gel. Interestingly, the rate of release of both MG and MH in this study is found to be negatively related to the mass percentage of CMC-Na (**Fig. 6B**), even though the latter is shown to be positively related to the swelling capacity of the fiber. This suggests that factors (including the affinity of drug molecules to the gel matrix) other than the degree of swelling play a role in determining the overall drug release pattern attained by the present gel system. Despite this, the release rate of drug molecules is still tunable by changing the mass percentage of CMC-Na in the fiber.

With the use of a dual-barrel syringe, a complex fiber with the Janus morphology can be fabricated from a co-flow of polymer blends with high viscosity (**Fig. 6C**). The composition of each of the fiber compartments can be changed simply by altering the mass-to-mass ratio of Na-Alg and CMC-Na. This allows the drug release rate in each of the compartments to be tuned precisely and individually. As shown in **Fig. 6D**, when MG and MH are loaded into the C-A1C0 compartment and the C-A1C3 compartment, respectively, of a complex fiber, the release rate of MG is significantly higher than that of MH, with almost 80% of MG released after the first 8 h when only 20% of MH is released. This release pattern can be changed in a way that both of the

loaded drugs are released at almost the same rate when the composition of the MG-loaded compartment is changed to C-A1C3 whereas that of the MH-loaded compartment is replaced with C-A1C0. This demonstrates the possibility of manipulating the composition of individual compartments to control the release patterns of co-delivered agents. Finally, the ability of the complex fiber to retain the activity of the loaded drug is determined based on the capacity of MH-loaded C-AxCy gels in inhibiting the growth of *Staphylococcus aureus* (gram-positive bacteria) and *Escherichia coli* (gram-negative bacteria). A zone of inhibition is observed in plates containing MH-loaded samples but not in those containing blank gels (**Fig. 7**). This reveals that encapsulation by C-AxCy has no significant influence on the activity of the loaded drug, and further corroborates the possible use of the complex fiber in multidrug therapy.

4. Conclusions

The use of multiple drugs for the treatment of a single disease has gained increasing interest in the literature due to its potential to attain a therapeutic effect that can hardly be achieved by using a single drug. To streamline the administration of a multi-drug regimen, complex fibers with the Janus morphology are fabricated and characterized in this study as drug carriers. By using CMC-Na as a modifier to manipulate the properties of different fiber compartments, the release rate of each of the co-delivered drugs can be precisely controlled to meet the needs of different multi-drug regimens. Apart from this, the process of drug loading is mediated solely by physical encapsulation under an all-aqueous environment, with no photochemical or chemical triggering required. This avoids the introduction of toxic organic residues into the fiber and prevents the induction of structural changes experienced by the loaded drug. Here it is worth mentioning that although only MG and MH are used in this study to

examine the performance of the fiber, due to the non-chemical nature of the drug loading method, the same approach can be translated into other drugs without being affected much by the chemical structure of drug molecules. Along with their ease of fabrication, the complex fibers reported in this study warrant further development for applications in which co-delivery of multiple agents is required.

Declaration of interest

The authors report no conflicts of interest. The authors alone are responsible for the content and writing of this article.

Acknowledgements

The authors would like to acknowledge Guoxing Deng and Yau-Foon Tsui for helpful comments and suggestions during the writing of this manuscript. Thanks are extended to funding support from Natural Science Foundation of Guangdong Province (2018A030310485) and the Chinese University of Hong Kong, Shenzhen (PF01001421).

References

1. Norouzi M, Nazari B, Miller DW. Injectable hydrogel-based drug delivery systems for local cancer therapy. Drug Discov Today 2016;21:1835-49.
2. Henderson PW, Singh SP, Krijgh DD, Yamamoto M, Rafii DC, Sung JJ, et al. Stromal-derived factor-1 delivered via hydrogel drug-delivery vehicle accelerates wound healing *in vivo*. Wound Repair Regen 2011;19:420-5.
3. Ren Y, Zhao X, Liang X, Ma PX, Guo B. Injectable hydrogel based on quaternized chitosan, gelatin and dopamine as localized drug delivery system to treat Parkinson's disease. Int J Biol Macromol 2017;105:1079-87.
4. Zhang S, Ermann J, Succi MD, Zhou A, Hamilton MJ, Cao B, et al. An inflammation-targeting hydrogel for local drug delivery in inflammatory bowel disease. Sci Transl Med. 2015;7:300ra128.
5. Lai WF, Susha AS, Rogach AL. Multicompartment microgel beads for co-delivery of multiple drugs at individual release rates. ACS Appl Mater Interfaces 2016;8:871-80.
6. Lai WF, Hu C, Deng G, Lui KH, Wang X, Tsoi TH, et al. A biocompatible and easy-to-make polyelectrolyte dressing with tunable drug delivery properties for wound care. Int J Pharm 2019;566:101-10.
7. Lai WF, Lin MC. Nucleic acid delivery with chitosan and its derivatives. J Control Release 2009;134:158-68.
8. Lai WF, He ZD. Design and fabrication of hydrogel-based nanoparticulate systems for *in vivo* drug delivery. J Control Release 2016;243:269-82.
9. Lai WF, Rogach AL, Wong WT. One-pot synthesis of an emulsion-templated hydrogel-microsphere composite with tunable properties. Compos Part A-Appl S 2018;113:318-29.

10. Lai WF, Lin MC. Folate-conjugated chitosan-poly(ethylenimine) copolymer as an efficient and safe vector for gene delivery in cancer cells. Curr Gene Ther 2015;15:472-80.
11. Alencastre JB, Bentley MVLB, Garcia FS, de Moragas M, Viladot JL, Marchetti JM. A study of the characteristics and *in vitro* permeation properties of CMC/ chitosan microparticles as a skin delivery system for vitamin E. Rev Bras Cienc Farm 2006;42:69-76.
12. Lai WF, Shum HC. A stimuli-responsive nanoparticulate system using poly(ethylenimine)-graft-polysorbate for controlled protein release. Nanoscale 2015;8:517-28.
13. Wang W, Hui PC, Wat E, Ng FS, Kan CW, Wang X, et al. *In vitro* drug release and percutaneous behavior of poloxamer-based hydrogel formulation containing traditional Chinese medicine. Colloids Surf B Biointerfaces 2016;148:526-32.
14. Uyen NTT, Hamid ZAA, Tram NXT, Ahmad N. Fabrication of alginate microspheres for drug delivery: a review. Int J Biol Macromol 2020;153:1035-46.
15. Severino P, da Silva CF, Andrade LN, de Lima Oliveira D, Campos J, Souto EB. Alginate nanoparticles for drug delivery and targeting. Curr Pharm Des 2019;25:1312-34.
16. Aderibigbe BA, Buyana B. Alginate in wound dressings. Pharmaceutics 2018;10:42.
17. Rabille H, Torode TA, Tesson B, Le Bail A, Billoud B, Rolland E, Le Panse S, Jam M, Charrier B. Alginates along the filament of the brown alga Ectocarpus help cells cope with stress. Sci Rep 2019;9:12956.
18. George M, Abraham TE. Polyionic hydrocolloids for the intestinal delivery of

protein drugs: alginate and chitosan - a review. J Control Release 2006;114:1-14.

19. Tilakaratne HK, Hunter SK, Andracki ME, Benda JA, Rodgers VG. Characterizing short-term release and neovascularization potential of multi-protein growth supplement delivered via alginate hollow fiber devices. Biomaterials 2007;28:89-98.
20. Hoesli CA, Luu M, Piret JM. A novel alginate hollow fiber bioreactor process for cellular therapy applications. Biotechnol Prog 2009;25:1740-51.
21. Liu Y, Sakai S, Taya M. Engineering tissues with a perfusable vessel-like network using endothelialized alginate hydrogel fiber and spheroid-enclosing microcapsules. Heliyon 2016;2:e00067.
22. Shao X, Hunter CJ. Developing an alginate/chitosan hybrid fiber scaffold for annulus fibrosus cells. J Biomed Mater Res A 2007;82:701-10.
23. Liu L, Jiang L, Xu GK, Ma C, Yang XG, Yao JM. Potential of alginate fibers incorporated with drug-loaded nanocapsules as drug delivery systems. J Mater Chem B. 2014;2:7596-604.
24. Vigani B, Rossi S, Sandri G, Bonferoni MC, Milanesi G, Bruni G, et al. Coated electrospun alginate-containing fibers as novel delivery systems for regenerative purposes. Int J Nanomedicine 2018;13:6531-50.
25. Shigeki S, Murakami T, Tani Y, Ikuta Y. Use of Sorbsan, a calcium alginate fiber dressing, as a drug reservoir in iontophoretic transdermal delivery. Plast Reconstr Surg 1998;102:2509-11.
26. Gong X, Dang G, Guo J, Liu Y, Gong Y. A sodium alginate/feather keratin composite fiber with skin-core structure as the carrier for sustained drug release. Int J Biol Macromol 2020;155:386-92.
27. Tian XY, Liu L. Drug discovery enters a new era with multi-target intervention

strategy. Chin J Integr Med 2012;18:539-42.

28. Larsson M, Huang WT, Liu DM, Losic D. Local co-administration of gene-silencing RNA and drugs in cancer therapy: state-of-the art and therapeutic potential. Cancer Treat Rev 2017;55:128-35.
29. Agoni C, Ramharack P, Soliman MES. Synergistic interplay of the co-administration of rifampin and newly developed anti-TB drug: could it be a promising new line of TB therapy? Comb Chem High Throughput Screen 2018;21:453-60.
30. Adeyemi WJ, Olayaki LA, Abdussalam TA, Fabiyi TO, Raji TL, Adetunji AA. Co-administration of omega-3 fatty acids and metformin showed more desirable effects than the single therapy on indices of bone mineralisation but not gluco-regulatory and antioxidant markers in diabetic rats. Biomed Pharmacother 2020;121:109631.
31. Cho H, Lai TC, Tomoda K, Kwon GS. Polymeric micelles for multi-drug delivery in cancer. AAPS PharmSciTech 2015;16:10-20.
32. Shin HC, Alani AW, Rao DA, Rockich NC, Kwon GS. Multi-drug loaded polymeric micelles for simultaneous delivery of poorly soluble anticancer drugs. J Control Release 2009;140:294-300.
33. He C, Lu K, Liu D, Lin W. Nanoscale metal-organic frameworks for the co-delivery of cisplatin and pooled siRNAs to enhance therapeutic efficacy in drug-resistant ovarian cancer cells. J Am Chem Soc 2014;136:5181-4.
34. Liu S, Zhao M, Zhou Y, Li L, Wang C, Yuan Y, et al. A self-assembling peptide hydrogel-based drug co-delivery platform to improve tissue repair after ischemia-reperfusion injury. Acta Biomater 2020;103:102-14.
35. Salmaso S, Semenzato A, Bersani S, Matricardi P, Rossi F, Caliceti P.

Cyclodextrin/PEG based hydrogels for multi-drug delivery. Int J Pharm 2007;345:42-50.

36. Molla MM, Alamgir Hossain M, Nasrin TAA, Islam MN, Sheel S. Study on preparation of shelf stable ready to serve (RTS) beverages based on bael pul. Bangladesh J Agric Res 2007;32:573-86.
37. Leonel AG, Mansur HS, Mansur AAP, Caires A, Carvalho SM, Krambrock K, et al. Synthesis and characterization of iron oxide nanoparticles/carboxymethyl cellulose core-shell nanohybrids for killing cancer cells *in vitro*. Int J Biol Macromol 2019;132:677-91.
38. Varma DM, Gold GT, Taub PJ, Nicoll SB. Injectable carboxymethylcellulose hydrogels for soft tissue filler applications. Acta Biomater 2014;10:4996-5004.
39. Patel MA, AbouGhaly MH, Schryer-Praga JV, Chadwick K. The effect of ionotropic gelation residence time on alginate cross-linking and properties. Carbohydr Polym 2017;155:362-71.
40. Dutta S, Samanta P, Dhara D. Temperature, pH and redox responsive cellulose based hydrogels for protein delivery. Int J Biol Macromol 2016;87:92-100.
41. Lai WF, Susha AS, Rogach AL, Wang GA, Huang MJ, Hu WJ, et al. Electrospray-mediated preparation of compositionally homogeneous core-shell hydrogel microspheres for sustained drug release. RSC Adv 2017;7:44482-91.
42. Shen SC, Ng WK, Shi Z, Chia L, Neoh KG, Tan RB. Mesoporous silica nanoparticle-functionalized poly(methyl methacrylate)-based bone cement for effective antibiotics delivery. J Mater Sci Mater Med 2011;22:2283-92.
43. Kwon C, Choi Y, Jeong D, Kim JG, Choi JM, Chun S, et al. Inclusion complexation of naproxen with cyclosophoraoses and succinylated cyclosophoraoses in different pH environments. J Incl Phenom Macro

2012;74:325-33.

44. Hettiarachchi G, Nguyen D, Wu J, Lucas D, Ma D, Isaacs L, et al. Toxicology and drug delivery by cucurbit[n]uril type molecular containers. PloS one 2010;5:e10514.

45. Mellott MB, Searcy K, Pishko MV. Release of protein from highly cross-linked hydrogels of poly(ethylene glycol) diacrylate fabricated by UV polymerization. Biomaterials 2001;22:929-41.

46. Lee JW, Kim SY, Kim SS, Lee YM, Lee KH, Kim SJ. Synthesis and characteristics of interpenetrating polymer network hydrogel composed of chitosan and poly(acrylic acid). J Appl Polym Sci 1999;73:113-20.

47. Zhang ZP, Feng SS. Nanoparticles of poly(lactide)/vitamin E TPGS copolymer for cancer chemotherapy: synthesis, formulation, characterization and *in vitro* drug release. Biomaterials 2006;27:262-70.

48. Alderman DJ, Clifton-Hadley RS. Malachite green: a pharmacokinetic study in rainbow trout, Oncorhynchus mykiss (Walbaum). J Fish Dis 1993;16:297-311.

49. White SW, Besanceney C. Systemic pigmentation from tetracycline and minocycline therapy. Arch Dermatol 1983;119:1-2.

Figure legends

Fig. 1. A schematic diagram showing the procedures for generating a complex fiber with the Janus morphology

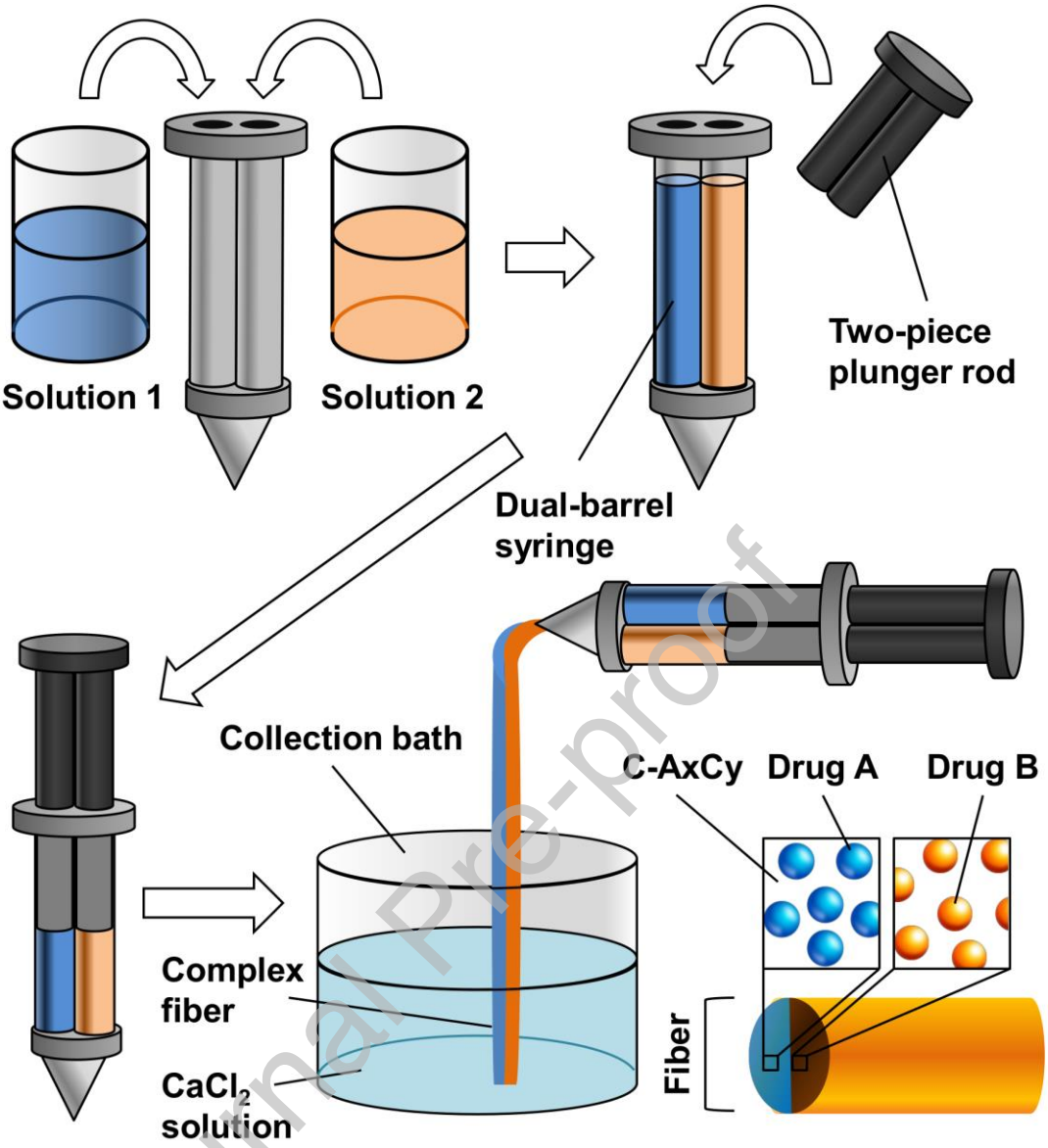

Fig. 2. (A) The viability of 3T3 mouse fibroblasts and HEK293 cells, as assessed by the MTS assay, after 5-h treatment with different concentrations of Na-Alg and CMC-Na, (a) without or (b) with a subsequent 24-h post-treatment incubation. Data are presented as the means ± SD of triplicate experiments. (B) The impact of 5-h treatment with different concentrations of Na-Alg and CMC-Na, (a) without or (b) with a subsequent 24-h post-treatment incubation, on the proliferation of 3T3 mouse fibroblasts and HEK293 cells as assessed by cell counting. Data are presented as the means ± SD of triplicate experiments. (C) Hemolytic rates of erythrocytes with increasing concentrations of different complex fibers. (D) TG curves of Na-Alg, CMC-Na, and the C-A1C3 fiber.

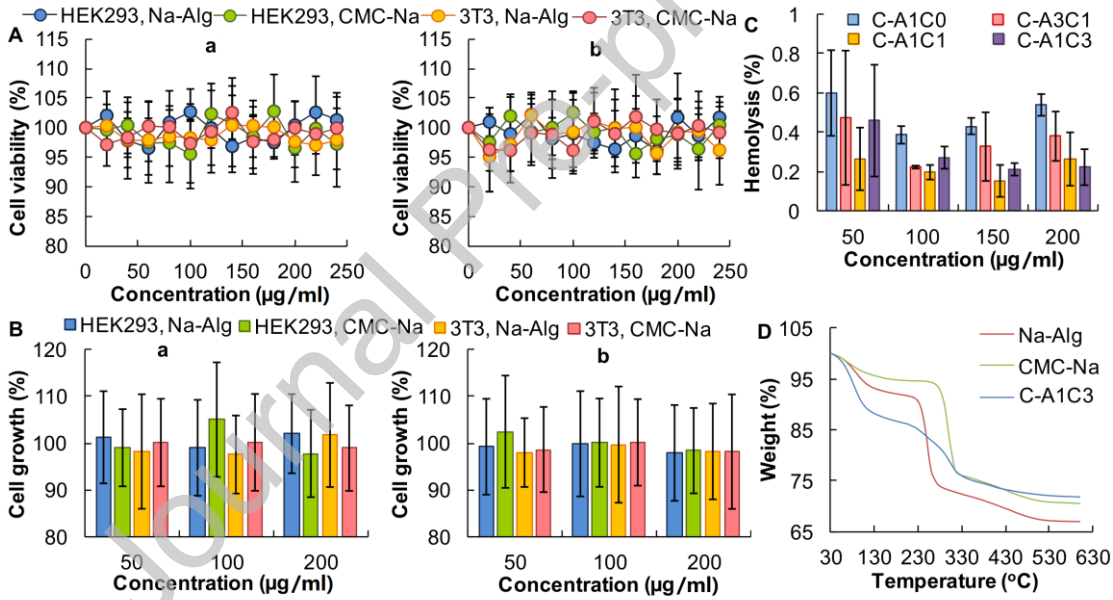

Fig. 3. (A) SEM micrographs of the cross-sections of complex fibers consisting of (a) C-A1C0, (b) C-A3C1, (c) C-A1C1, and (d) C-A1C3. Scale bar = 500 μm. (B) Tensile stress-strain curves of different complex fibers. (C) The viscosity of different Na-Alg/CMC-Na blends at shear rates from 0 to 1 s^{-1}. (D) The G' values and (E) G'' values of different complex fibers at angular frequencies from 0.1 to 100 rad/s.

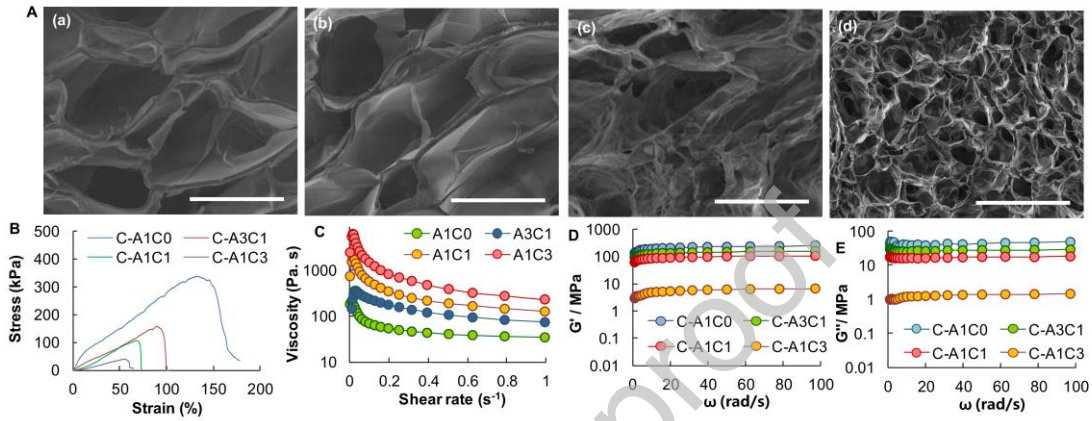

Fig. 4. (A) The swelling capacity of different complex fibers in simulated body fluid. Data are presented as the means ± SD of triplicate experiments. (B) The water content of fibers consisting of (i) C-A1C0, (ii) C-A3C1, (iii) C-A1C1, and (iv) C-A1C3. Data are presented as the means ± SD of triplicate experiments (*P < 0.05).

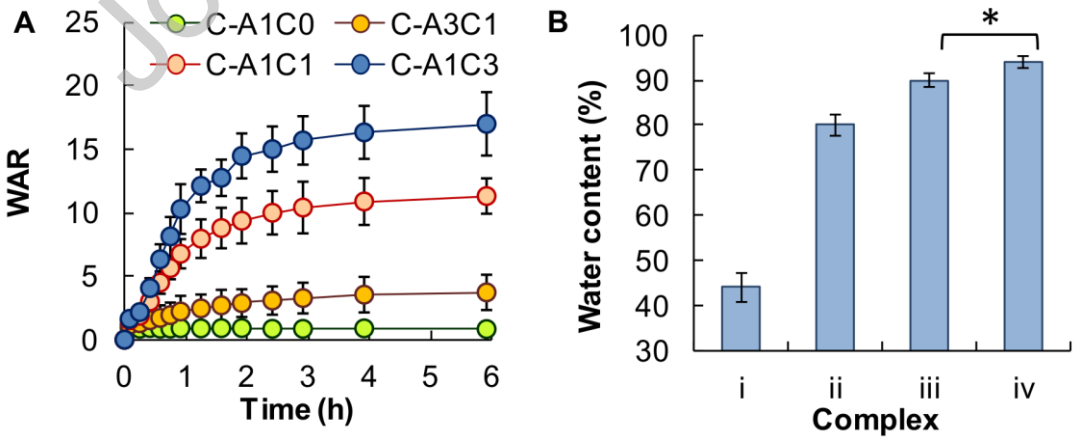

Fig. 5. (A) UV-vis spectra of MG and MH. (B) The EE of C-A1C1 fibers with different diameters. Data are presented as the means ± SD of triplicate experiments. (C) The profiles of release of (a) MG and (b) MH from C-A1C1 fibers with different diameters. Data are presented as the means ± SD of triplicate experiments.

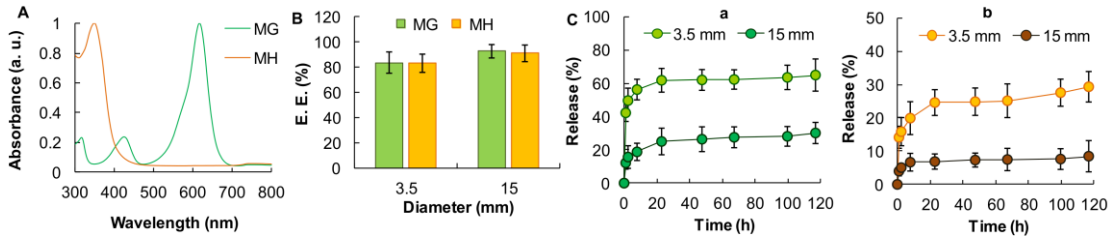

Fig. 6. (A) The EE of fibers with different mass percentages of CMC-Na. Data are presented as the means ± SD of triplicate experiments. (B) The profiles of release of (a) MG and (b) MH from fibers with different mass percentages of CMC-Na. Data are presented as the means ± SD of triplicate experiments. (C) (a) An optical image of a complex fiber with the Janus morphology, as well as (b) a magnified view of the cross-sectional area of a segment of the fiber. To enhance easy recognition of the Janus morphology, one of the compartments is stained with Congo red. (D) The profiles of release of MG and MH from a complex fiber with the Janus morphology: (a) C-A1C0 compartment for MG and C-A1C3 compartment for MH, and (b) C-A1C3 compartment for MG and C-A1C0 compartment for MH. Data are presented as the means ± SD

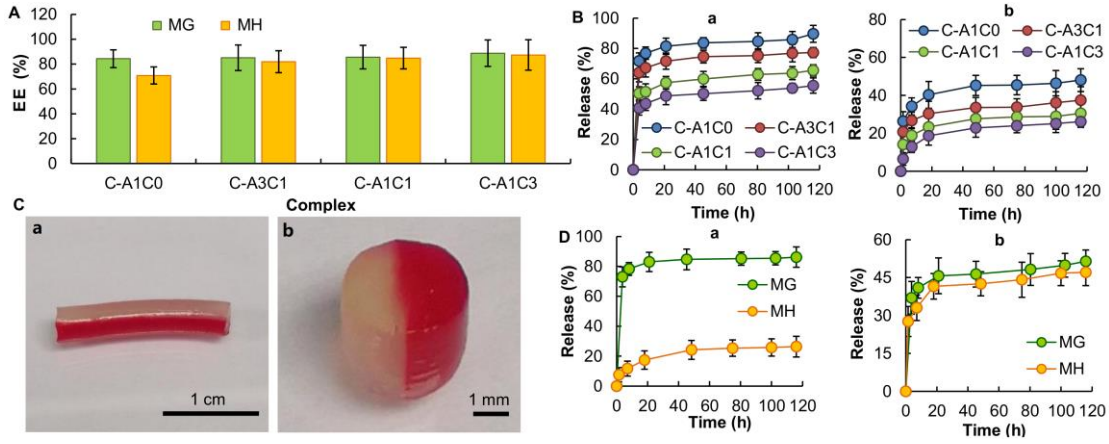

Fig. 7. (A) Images showing the zone of inhibition induced by (a, f) blank C-A1C1, (b, g) MH-loaded C-A1C0, (c, h) MH-loaded C-A3C1, (d, i) MH-loaded C-A1C1, and (e, j) MH-loaded C-A1C3 for (a-e) *E. coli* and (f-j) *S. aureus*. Scale bar = 2 cm. (B) Area percentages of the zone of inhibition induced by different MH-loaded gels for (a) *E. coli* and (b) *S. aureus*. Data are presented as the means ± SD of triplicate experiments.